Supporting information

Isomerizing Thieno[3,4-b]thiophene-Based Near-Infrared Non-fullerene Acceptors towards High-Performance Organic Solar Cells

Zeqi Zhang, Tong Shan, Yi Zhang, Lei Zhu, Lingwei Kong, Feng Liu and Hongliang Zhong*

School of Chemistry and Chemical Engineering, Shanghai Key Lab of Electrical Insulation and Thermal Aging, Shanghai Jiao Tong University, Shanghai 200240, P. R. China.

E-mail: hlzhong@sjtu.edu.cn

Materials

All the reagents are purchased from commercial resource and used without further purification. Solvents for reactions are freshly distilled prior to use.

Instruments

^{1}H and ^{13}C NMR spectra were recorded on a Bruker AV-400 (400 MHz) or a Bruker Advanced III (500 MHz) spectrometers, using the residual solvent resonance of $CDCl_3$ or TMS as an internal reference and are given in ppm. UV-Vis absorption spectra were measured by a PerkinElmer Lambda 750S recording spectrophotometer. Cyclic voltammetry (CV) measurements of targeted SMAs thin films were conducted on a CHI660D voltammetric analyzer in acetonitrile solution with 0.1M tetrabutylammonium hexafluorophosphate (n-Bu_4NPF_6) as supporting electrolyte at room temperature by using conventional three-electrode configuration consisting of a platinum working electrode, a platinum wire counter electrode and a Ag/AgCl wire reference electrode. Current J-V curves for organic solar cells were measured at room temperature by using a Keithley 2420 SourceMeter. The charge mobility was measured by the space charge-limited current (SCLC) method with a hole-only device configuration (ITO/PEDOT:PSS/Active layer/MoO_3/Al) for hole mobility and an electron-only device configuration (ITO/ZnO/Active layer/Ca/Al) for electron mobility. Both hole and electron mobilities were extracted by fitting measured *J-V* curves using the empirical Mott-Gurney formula in single carrier SCLC device with the equation of $\ln(JL^3/V^2) \approx 0.89(1/E_0)^{0.5} (V/L) + \ln(9\varepsilon_0\varepsilon_r\mu/8)$. Grazing-incidence wide-angle x-ray scattering (GIWAXS) was carried out at beamline 7.3.3 Lawrence Berkeley National Lab (LBNL). The sample was put inside a helium chamber, and Pilatus 2M detector was used to collect the signal. GIWAXS raw data were analyzed using Nika software package and peak information was assessed by Gaussian fitting.

Device Fabrication

The patterned indium tin oxide glass (ITO) glass substrates (sheet resistance = 15 Ω sq^{-1}) were cleaned in detergent, de-ion water, acetone, chloroform, acetone, and isopropanol sequentially by ultra-sonic bath for 15 min each and then dried by N_2 gas. Further UV-Ozone treatment for 5 min was applied before use.

The ZnO precursor solution was prepared by dissolving zinc acetate dihydrate ($Zn(CH_3COO)_2 \bullet 2H_2O$, Sigam-Aldrich, 99.0%, 1 g) and ethanolamine ($NH_2CH_2CH_2OH$, Acros, 99 %, 0.28 g) in 2-methoxyethanol ($CH_3OCH_2CH_2OH$, Aladdin, 99.8%, 10 mL) under vigorous stirring for 15 h for the hydrolysis reaction and aging in air. The ZnO precursor solution was spin-cast on top of the ITO-glass substrate. The films were annealed at 200 °C for 20 min in air to form thickness of approximately 35 nm determined by an AFM. Then the ZnO-coated substrates were transferred into a nitrogen-filled glove box. In order to fine tune the interfacial properties, a thin film of poly[(9,9-bis(3'-(*N*,*N*-dimethyl)-nethylammoinium-propyl)-2,7-fluorene)-*alt*-2,7-(9,9-dioctylfluorene)] (PFN) film (ca. 5 nm) was prepared by spin-coating PFN solution (0.4 mg/mL in methanol) onto ZnO. The PTB7-Th : acceptor blends were dissolved in CF with 1 V% 1-chloronaphthalene (CN) as additive at 40 ℃ and stirred overnight in a nitrogen-filled glove box. The active layers with optimized thicknesses (ca. 100 nm) were obtained by spin-coating the blend solution at room temperature with polymer concentrations of 9.5 mg mL^{-1} that was filtered by a PTFE (polytetrafluoroethylene) filter (pore size of 0.45 μm) atop the PFN layer, and annealed at 110 °C for 10 min in glove box. Then, approximately 10 nm MoO_3 was evaporated on top of the active layer at a speed of 0.03 nm/s. Finally, the anode, 100 nm Al was deposited at a speed of 0.3 nm/s through a shadow mask by thermal evaporation in a vacuum chamber of under 3 $\times$ 10^{-6} Torr to complete the device fabrication. The active area of each device was 3.68 mm^2.

Synthesis

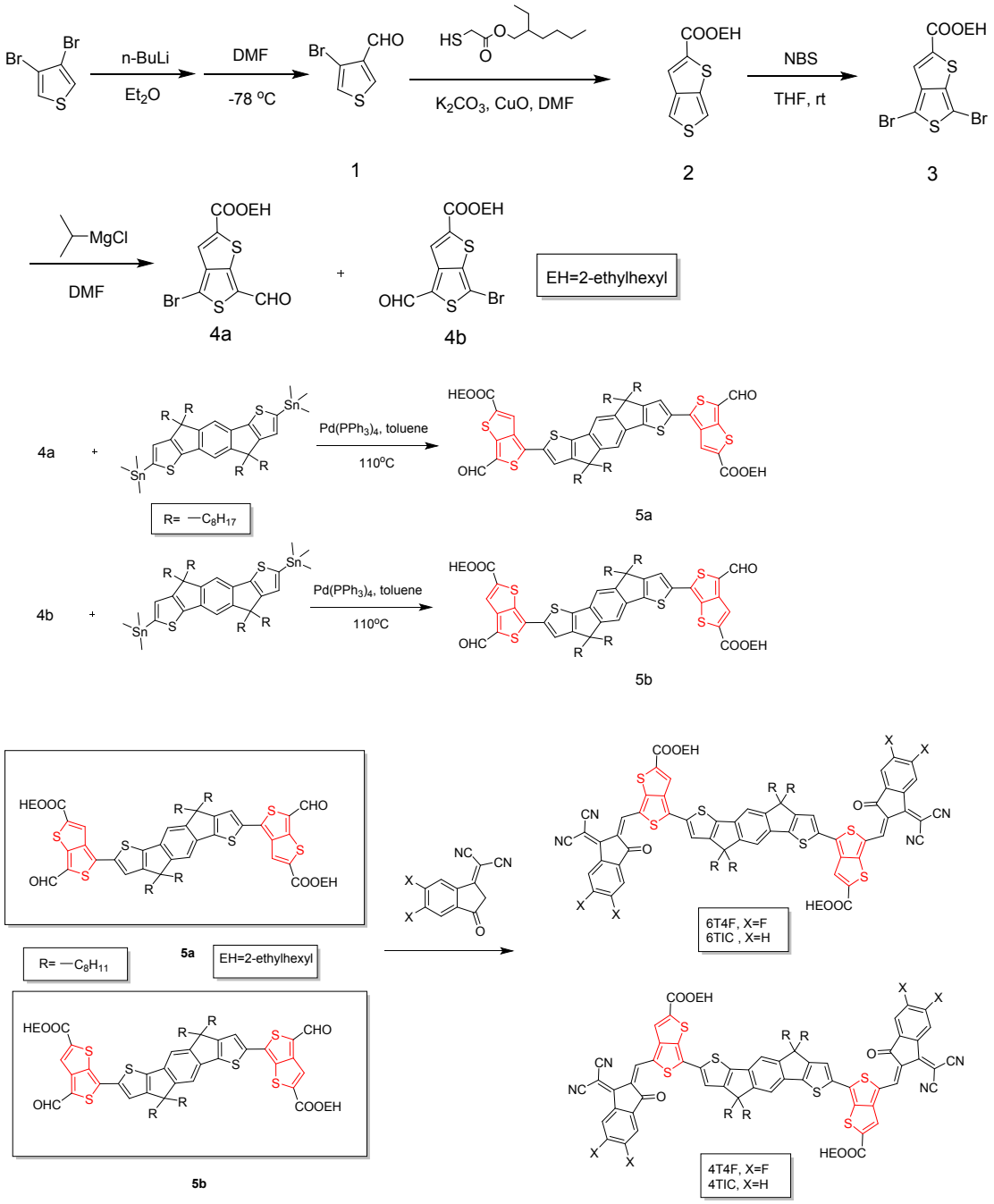

Scheme S1. Synthetic route for 4TIC, 4T4F, 6TIC and 6T4F.

Compound1,2, 3 were prepared according to the literature.[1]

2-ethylhexyl 4-bromo-6-formylthieno[3,4-b]thiophene-2-carboxylate (4a) and 2-ethylhexyl 6-bromo-4-formylthieno[3,4-b]thiophene-2-carboxylate (4b)

3 (2.1 g, 4.6 mmol) was added into 80 mL anhydrous THF under argon. The mixture was cooled to -78 ℃, followed by the addition of isopropylmagnesium chloride (0.57

g, 5.5 mmol) dropwise. After stirring for 30 minutes at -78 ℃, DMF (0.57 mL) was added slowly to the reaction mixture. The resulting solution was allowed to slowly warm to room temperature and kept stirring overnight. The reaction was then quenched by water and extracted with dichloromethane. The organic layer was then washed with water and brine, and then dried with Na_2SO_4. The solvent was removed under reduced pressure. Then the residue (~2:1 of mix **4a**:**4b**) was purified with silica gel chromatography to provide dark red solid **4a** (0.8 g, 43%) and dark yellow solid **4b** (0.34g, 18%).

4a: ^{1}H NMR (400 MHz, $CDCl_3$) δ 9.82 (s, 1H), 7.67 (s, 1H), 4.27 (d, *J* = 5.7 Hz, 2H), 1.72 (m, 1H), 1.4-1.32 (m, 8H), 0.97-0.90 (m, 6H).

4b: ^{1}H NMR (400 MHz, $CDCl_3$) δ 9.97 (s, 1H), 8.11 (s, 1H), 4.28 (d, *J* = 5.7 Hz, 2H), 1.72 (m, 1H), 1.49-1.32 (m, 8H), 0.97-0.90 (m, 6H).

Compound 5a

To a solution of **4a** (0.27 g, 0.67 mmol) and (4,4,9,9-tetraoctyl-4,9-dihydro-s-indaceno[1,2-b:5,6-b']dithiophene-2,7-diyl)bis(trimethylstannane) (0.32 g, 0.3 mmol) in dry toluene (10 mL), $Pd(PPh_3)_4$ (17 mg, 5% mmol) were added under argon. After stirring at 110 °C for 15 h, the mixture was cooled to room temperature and extracted with dichloromethane. The organic layer was then washed with water and brine, and then dried with Na_2SO_4. The final product was purified with silica gel chromatography to provide dark blue solid **5a** (0.26 g, 62%)**.**

5a: ^{1}H NMR (400 MHz, $CDCl_3$) δ 9.88 (s, 2H), 8.18 (s, 2H), 7.43 (s, 2H), 7.38 (s, 2H), 4.31 (m, 4H), 2.11-2.03 (m, 4H), 1.99-1.91 (m, 4H), 1.77-1.74 (m, 2H), 1.50-1.35 (m, 16H), 1.20-1.10 (m, 40H), 1.01-0.92 (m, 16H), 0.79 (m, 16H); ^{13}C NMR (100 MHz, $CDCl_3$) δ 178.70, 162.52, 157.08, 154.12, 147.11, 145.61, 140.93, 140.72, 140.39, 136.54, 136.00, 123.31, 122.74, 121.86, 113.97, 68.41, 54.56, 39.07, 38.91, 31.78, 30.51, 29.92, 29.29, 29.21, 28.99, 24.26, 23.94, 23.00, 22.60, 14.10, 14.05, 11.11. MS (MALDI-TOF) *m/z*: Calculated for $C_{80}H_{110}O_6S_6$ 1358.66; found: 1358.32.

Compound 5b

The synthesis of **5b** follows the same procedure as **5a**, using **4b** instead of **4a**. Final product was dark blue solid. (0.29 g, 64%).

5b: ^{1}H NMR (400 MHz, $CDCl_3$) δ 10.09 (s, 2H), 8.16 (s, 2H), 7.4 (d, *J*=1.1Hz, 4H), 4.35 (m, 4H), 2.10-2.04 (m, 4H), 2.01-1.92 (m, 4H), 1.84-1.78 (m, 2H), 1.55-1.34 (m, 16H), 1.15 (m, 40H), 1.04-0.93 (m, 16H), 0.82 (m, 16H); ^{13}C NMR (100 MHz, $CDCl_3$) δ 178.70, 162.52, 157.08, 154.12, 147.11, 145.61, 140.93, 140.72, 140.39, 136.54, 136.00, 123.31, 122.74, 121.86, 113.97, 68.41, 54.56, 39.07, 38.91, 31.78, 30.51, 29.92, 29.29, 29.21, 28.99, 24.26, 23.94, 23.00, 22.60, 14.10, 14.05, 11.11. MS (MALDI-TOF) *m/z*: Calculated for $C_{80}H_{110}O_6S_6$ 1358.66; found: 1358.31.

6T4F

5a (220 mg, 0.16 mmol), 2-(5,6-difluoro-3-oxo-2,3-dihydro-1H-inden-1-ylidene)malononitrile (82 mg, 0.36 mmol) and 1-butanol (20 ml) were added into a dry flask, then the mixture was heated to 110 ℃ and stirred overnight. The resulting mixture

was cooled to room temperature and filtered. The filter residue was washed with methanol, and then the crude product was purified on a silica-gel column chromatography to afford dark-green solid (194 mg, 67%). ^{1}H NMR (400 MHz, $CDCl_3$) δ 8.92 (s, 2H), 8.50 (dd, *J* = 10.0, 6.5 Hz, 2H), 8.23 (s, 2H), 7.73 (s, 2H), 7.65 (m, 2H), 7.47 (s, 2H), 4.33 (d, *J* = 6.0 Hz, 4H), 2.18-2.07 (m, 4H), 2.02 (m, 4H), 1.80 (m, 2H), 1.52-1.33 (m, 16H), 1.15 (m, 40H), 1.03-0.92 (m, 16H), 0.79 (m, 16H). ^{13}C NMR (125 MHz, $CDCl_3$) δ 186.75, 161.77, 159.59, 158.64, 157.24, 155.22, 153.35, 153.24, 153.13, 149.67, 148.45, 139.95, 137.14, 136.69, 134.18, 131.97, 124.37, 121.89, 118.67, 114.90, 114.69, 114.61, 112.34, 112.19, 68.91, 68.40, 39.18, 38.87, 31.79, 30.52, 29.93, 29.32, 29.25, 28.95, 24.36, 23.96, 23.01, 22.61, 14.13, 14.07, 11.09. MS (MALDI-TOF) *m/z*: Calculated for $C_{104}H_{114}F_4N_4O_6S_6$ 1782.70; found: 1782.50.

6TIC

5a (187 mg, 0.14 mmol), 2-(3-oxo-2, 3-dihydro-1H-inden-1-ylidene)malononitrile (59 mg, 0.3 mmol) and 1-butanol (20 ml) were added into a dry flask, then the mixture was heated to 110 ℃ and stirred for 6 hours. The resulting mixture was filtered, then the residue was washed with methanol. The crude product was purified on a silica-gel column chromatography to afford dark-green solid (180 mg, 77%). ^{1}H NMR (400 MHz, $CDCl_3$) δ 8.85 (s, 2H), 8.57-8.55 (m, 2H), 8.16 (s, 2H), 7.82 (dd, *J* = 5.3, 3.1 Hz, 2H), 7.75 (s, 2H), 7.68-7.60 (m, 4H), 7.48 (s, 2H), 4.32 (d, *J* = 6.0 Hz, 4H), 2.13-1.98 (m, 8H), 1.85-1.77 (m, 2H), 1.55-1.36 (m, 16H), 1.17 (m, 40H), 1.00 (m, 16H), 0.80 (m, 16H). ^{13}C NMR (100 MHz, $CDCl_3$) δ 189.37, 162.11, 159.45, 159.04 155.28, 158.66 149.18, 147.61, 140.34, 139.99, 136.82, 135.09, 134.18, 132.32, 132.06, 125.29, 124.57, 124.28, 123.52, 115.49, 115.20, 114.75, 69.03, 68.33, 39.43, 39.10, 32.02, 30.75, 30.20, 29.57, 29.50, 29.19, 24.61, 24.19, 23.24, 22.84, 14.36, 14.29, 11.33. MS (MALDI-TOF) m/z: Calculated for $C_{104}H_{118}N_4O_6S_6$ 1710.74; found: 1710.59.

4T4F

5b (202 mg, 0.15 mmol)， 2-(5,6-difluoro-3-oxo-2,3-dihydro-1H-inden-1-ylidene)malononitrile (75 mg, 0.33 mmol) and 1-butanol (20 ml) were added into a dry flask, then the mixture was heated to 110 °C and stirred for 6 hours. The resulting mixture was cooled to room temperature and filtered. The filter residue was washed with methanol, and then the crude product was purified on a silica-gel column chromatography to afford dark-green solid (190 mg, 72%). ^{1}H NMR (400 MHz, $CDCl_3$) δ 9.27 (s, 2H), 8.50 (m, 2H), 8.11 (s, 2H), 7.70 (s, 2H), 7.65 (m, 2H), 7.47 (s, 2H), 4.35 (d, *J* = 6.0 Hz, 4H), 2.10 (m, 4H), 2.01 (m, 4H), 1.83-1.74 (m, 2H), 1.54-1.33 (m, 16H), 1.14 (m, 40H), 1.04-0.92 (m, 16H), 0.81-0.78 (m, 16H). ^{13}C NMR (125 MHz, $CDCl_3$) δ 186.65, 162.01, 158.73, 158.05, 157.69, 155.03, 149.19, 146.17, 144.75, 137.00, 136.84, 136.77, 136.61, 136.52, 134.25, 132.11, 125.55, 123.62, 123.04, 118.78, 115.17, 115.02, 114.87, 114.59, 68.83, 68.23, 39.16, 38.93, 31.78, 30.49, 29.93, 29.30, 29.23, 29.03, 24.35, 23.92, 23.00, 22.61, 14.13, 14.07, 11.12. MS (MALDI-TOF) *m/z*: Calculated for $C_{104}H_{114}F_4N_4O_6S_6$ 1782.70; found: 1782.52.

4TIC

5b (180 mg, 0.13 mmol) and 2-(3-oxo-2,3-dihydro-1H-inden-1-ylidene)malononitrile (56 mg, 0.29 mmol) and 1-butanol (20 ml) were added into a dry flask, then the mixture was heated to 110 °C and stirred for 5 hours. The resulting mixture was cooled to room temperature and filtered. The filter residue was washed with methanol, and then the crude product was purified on a silica-gel column chromatography to afford dark-green solid (168 mg, 74%). ^{1}H NMR (400 MHz, $CDCl_3$) δ 9.32 (s, 2H), 8.70-8.65 (m, 2H), 8.14 (s, 2H), 7.91 (dd, *J* = 7.2, 1.6 Hz, 2H), 7.77-7.71 (m, 4H), 7.69 (s, 2H), 7.45 (s, 2H), 4.35 (d, *J* = 6.0 Hz, 4H), 2.11 (m, 4H), 2.04-1.96 (m, 4H), 1.79 (m, 2H), 1.53-1.30 (m, 16H), 1.24-1.09 (m, 40H), 1.03-0.91 (m, 16H), 0.79 (m, 16H). ^{13}C NMR (125 MHz, $CDCl_3$) δ 188.92, 162.07, 159.38, 158.56, 157.53, 154.92, 148.60, 145.54, 143.58, 140.12, 136.53, 136.16, 134.73, 133.90, 131.86, 125.83, 125.00, 123.34, 123.21, 123.07, 119.75, 115.52, 114.92, 114.47, 68.73, 67.97, 39.21, 38.95, 31.81, 30.50, 30.01, 29.37, 29.29, 29.06, 24.41, 23.94, 23.03, 22.63, 14.16, 14.08, 11.15. MS (MALDI-TOF) *m/z*: Calculated for $C_{104}H_{118}N_4O_6S_6$ 1710.74; found: 1710.63.

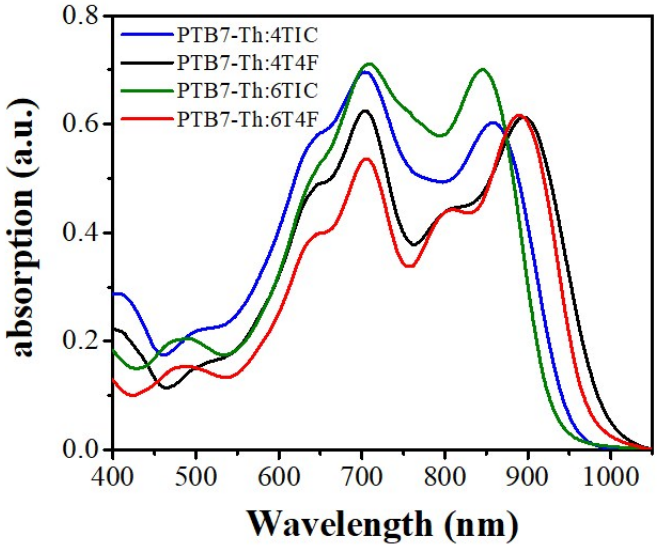

Fig. S1 The normalized UV-Vis-NIR absorption spectra of the optimal PTB7-Th:acceptors devices.

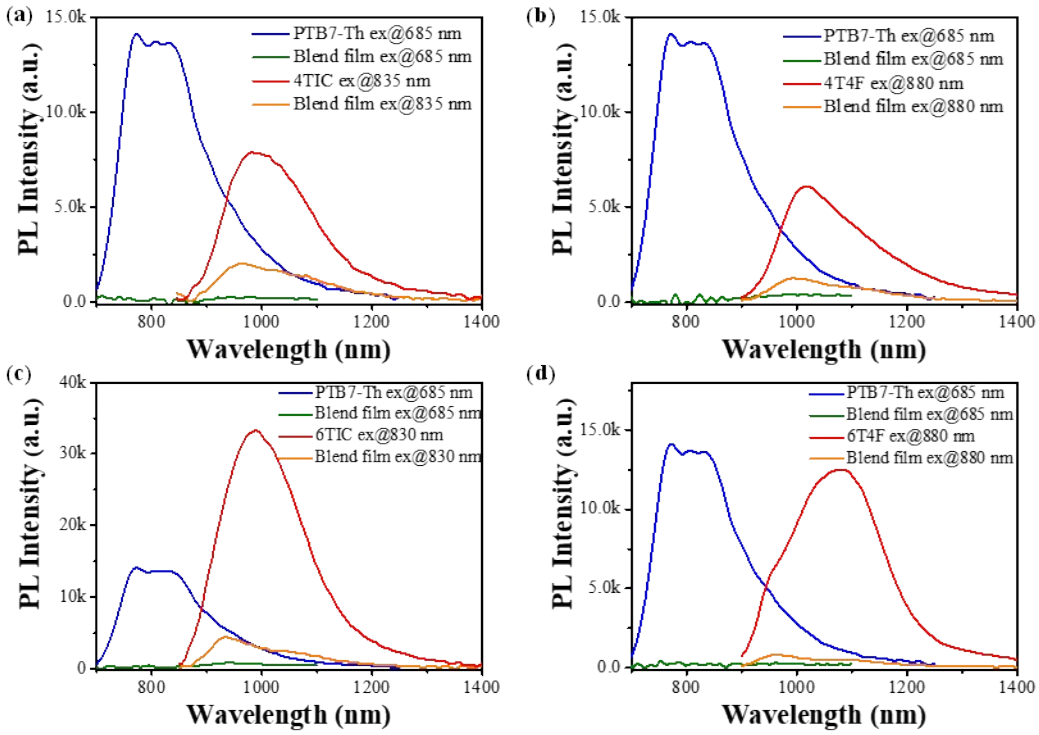

Fig. S2 Photoluminescence spectral of 4TIC (a, excited at 835 nm), 4T4F (b, excited at 880 nm), 6TIC (c, excited at 830 nm), 6T4F (d, excited at 880 nm) and PTB7-Th (excited at 685 nm) neat films as well as PTB7-Th:acceptors films excited at corresponding wavelength.

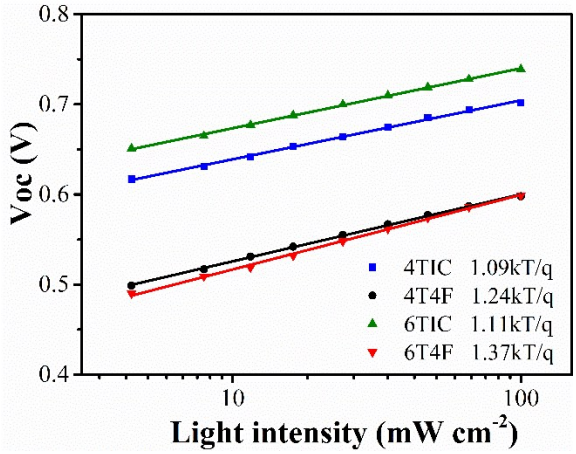

Fig. S3. Variation of V_{oc} with light intensity for the OSCs based on different acceptors.

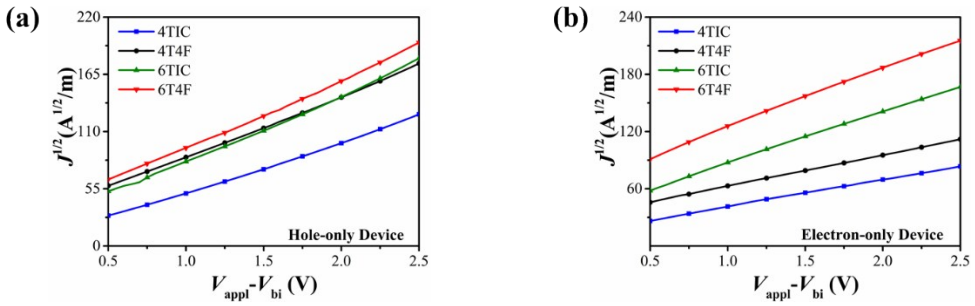

Fig. S4. $J^{1/2}$-V plots of (a) hole-only devices based on PTB7-Th:acceptors blends and (b) the electron-only devices based on PTB7-Th:acceptors blends under the optimized conditions.

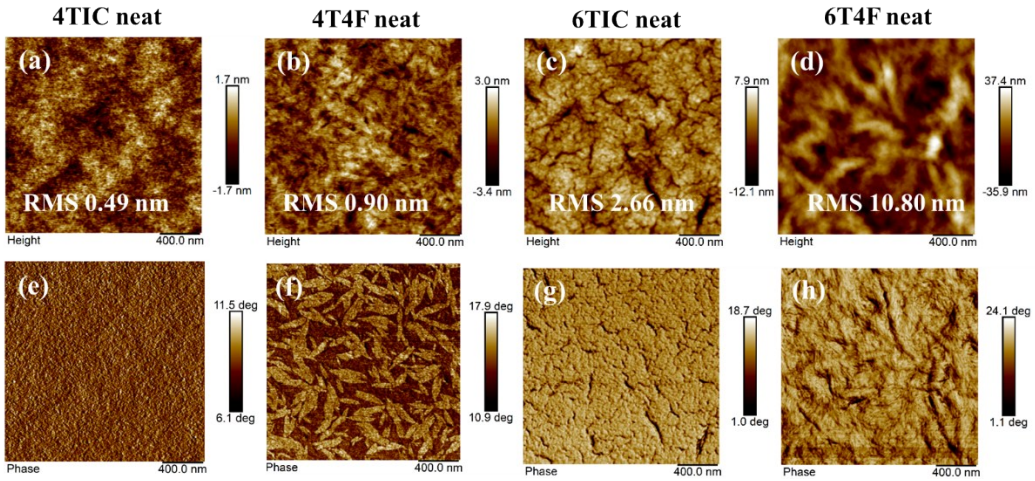

Fig. S5 AFM height and phase images of 4TIC (a, e), 4T4F (b, f), 6TIC (c, g) and 6T4F (d, h) neat films.

Table S1 Characteristic length scale of packing phenomenon for blend films of PTB7-Th:acceptors.

Blend	Lamellar				π-Stacking			
	q [Å^{-1}]	(100) distance [Å]	FWHM[a)] [Å^{-1}]	CCL[b)] [Å]	q [Å^{-1}]	π-π distance [Å^{-1}]	FWHM[a)] [Å^{-1}]	CCL[b)] [Å]
PTB7-Th:4TIC	0.337	18.64	0.035	80.78	1.852	3.39	0.139	20.34
PTB7-Th:4T4F	0.337	18.64	0.032	88.36	1.868	3.36	0.129	21.92
PTB7-Th:6TIC	0.338	18.59	0.022	128.52	1.857	3.38	0.123	22.99
PTB7-Th:6T4F	0.338	18.59	0.026	108.75	1.870	3.36	0.127	22.26

a) FWHM represents full-width at half maximum; b) CCL represents crystal coherence length.

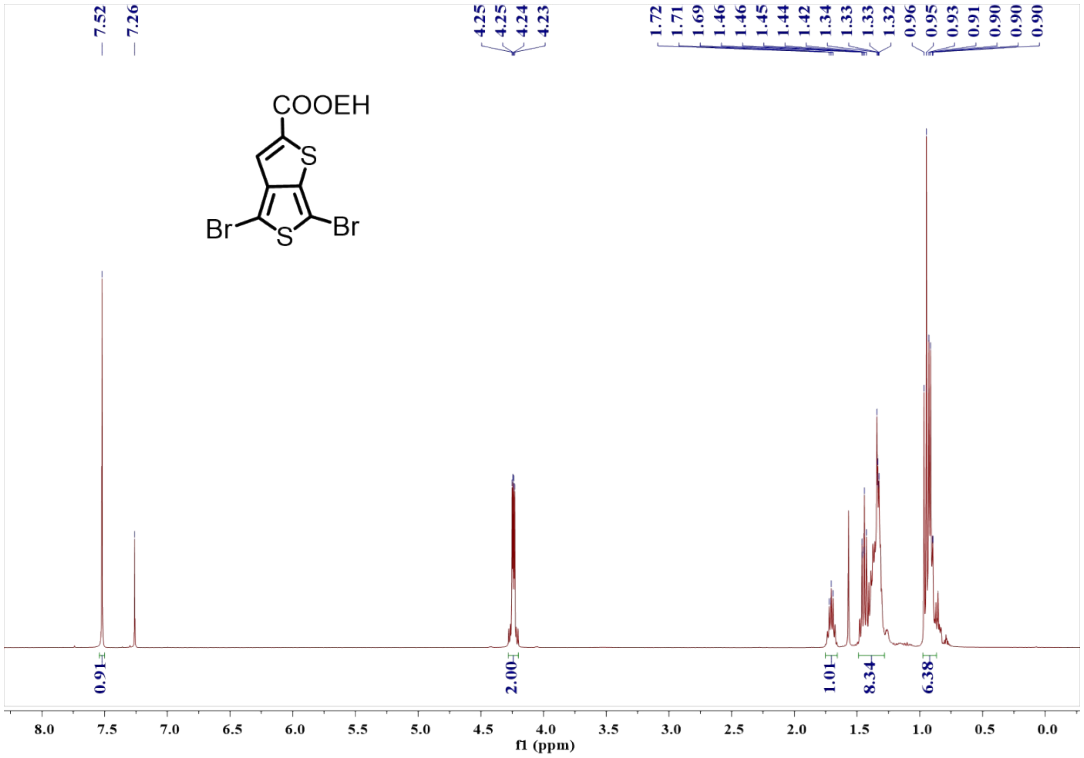

Fig. S6. [1]H NMR spectrum of **compound 3**.

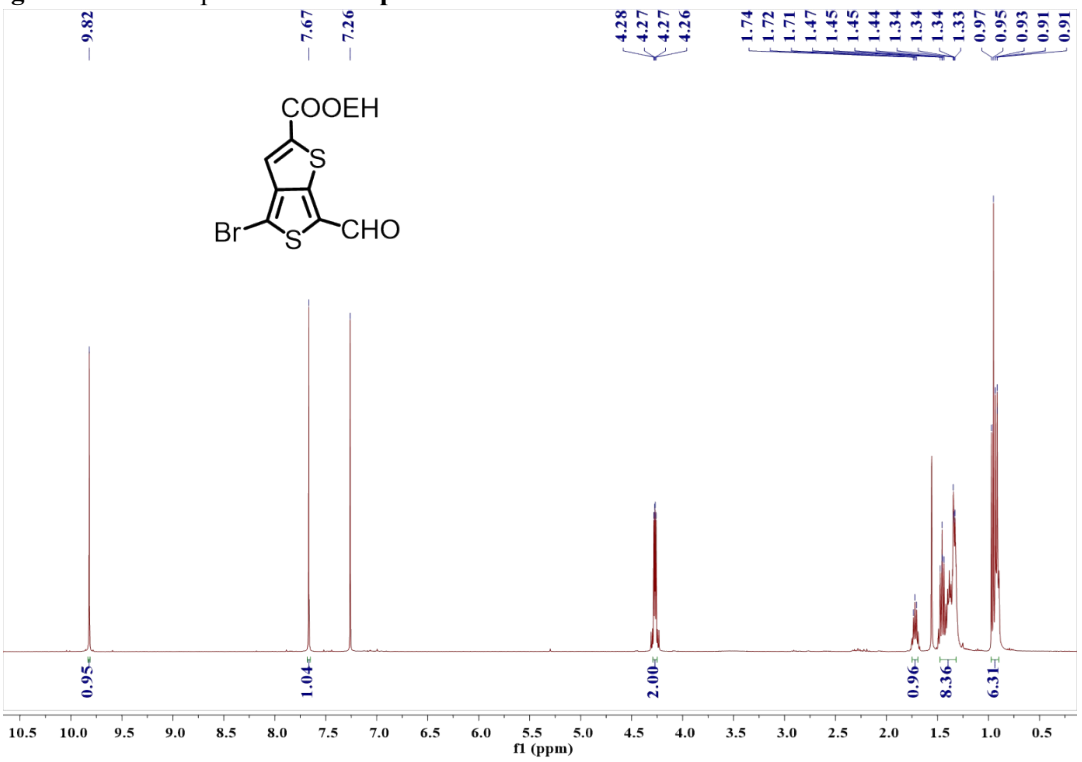

Fig. S7. [1]H NMR spectrum of **compound 4a**.

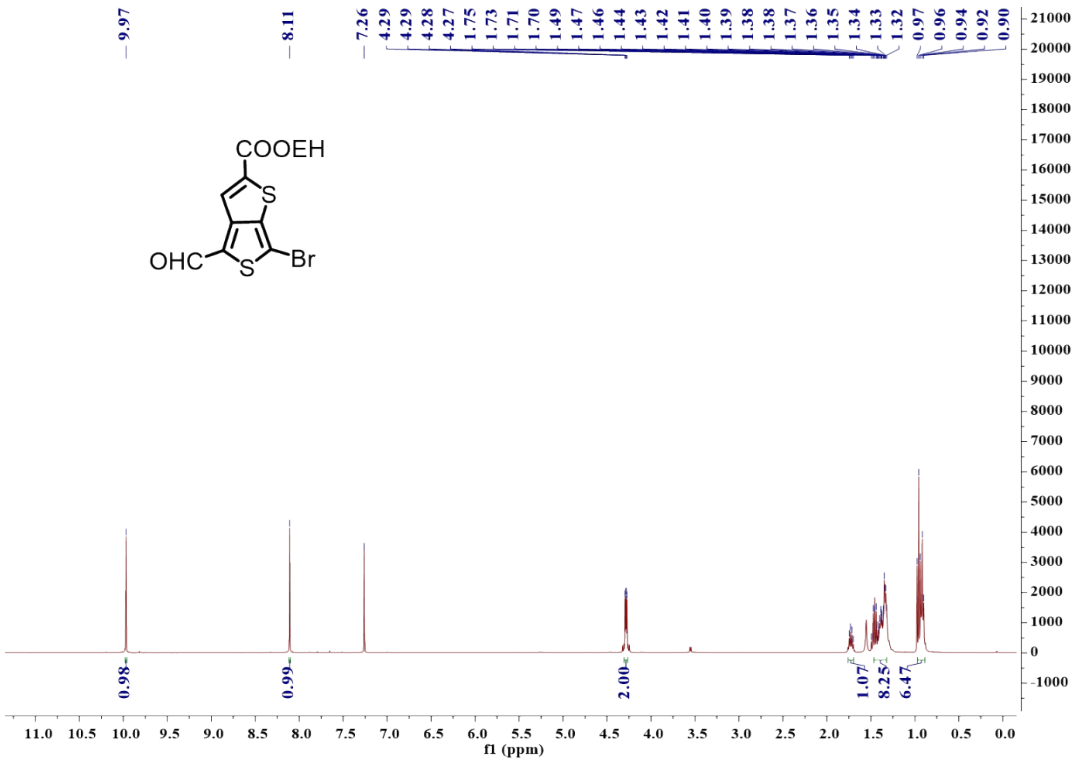

Fig. S8. [1]H NMR spectrum of **compound 4b**.

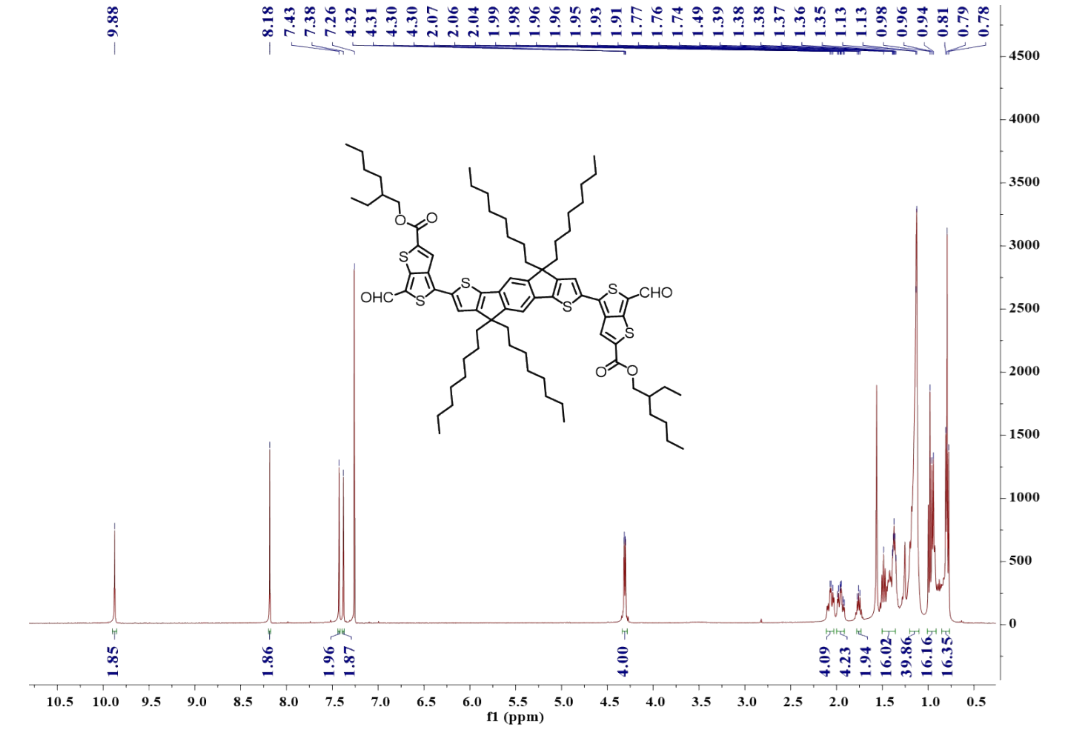

Fig. S9. [1]H NMR spectrum of **compound 5a**.

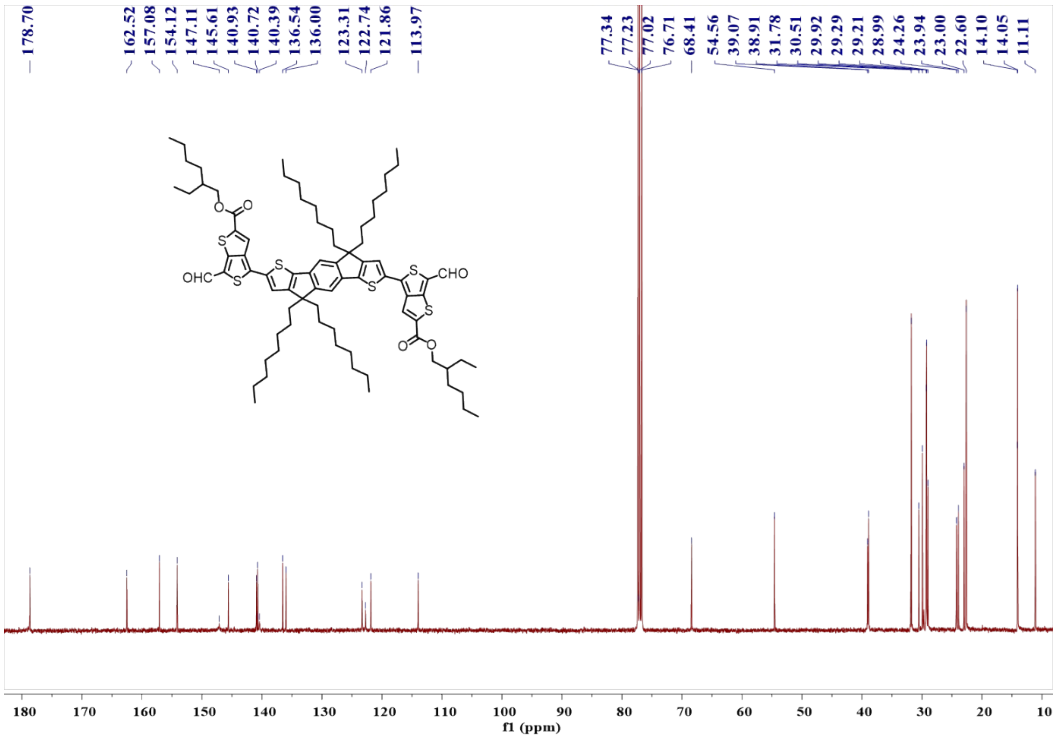

Fig. S10. ^{13}C NMR spectrum of **compound 5a**.

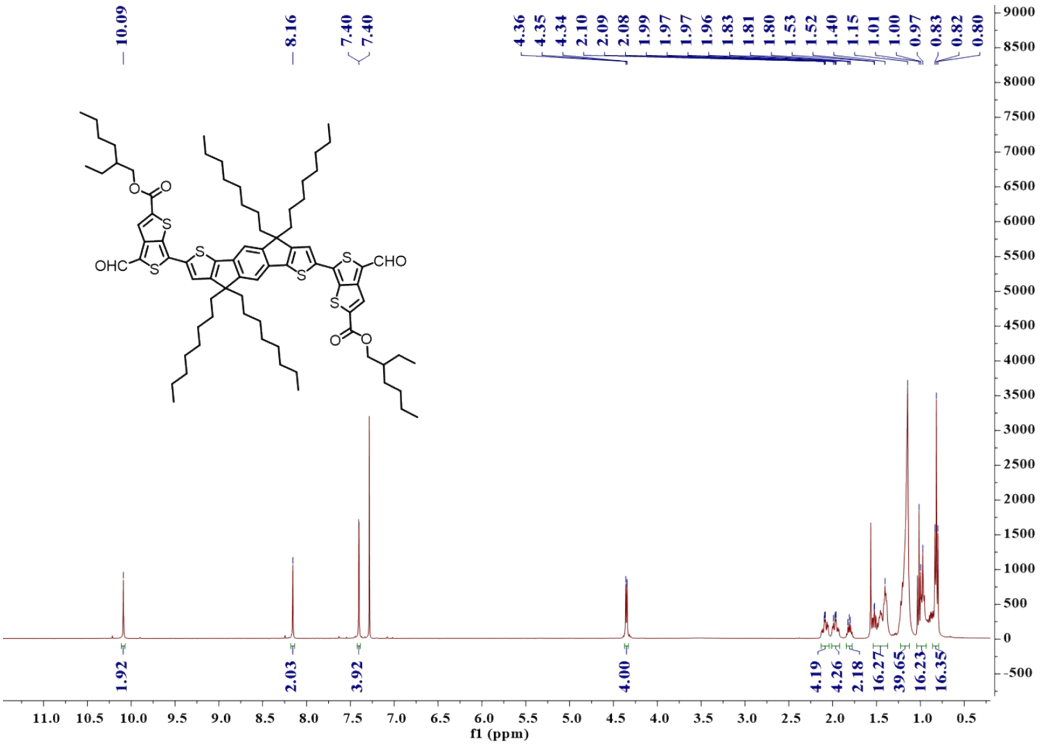

Fig. S11. ^{1}H NMR spectrum of **compound 5b**.

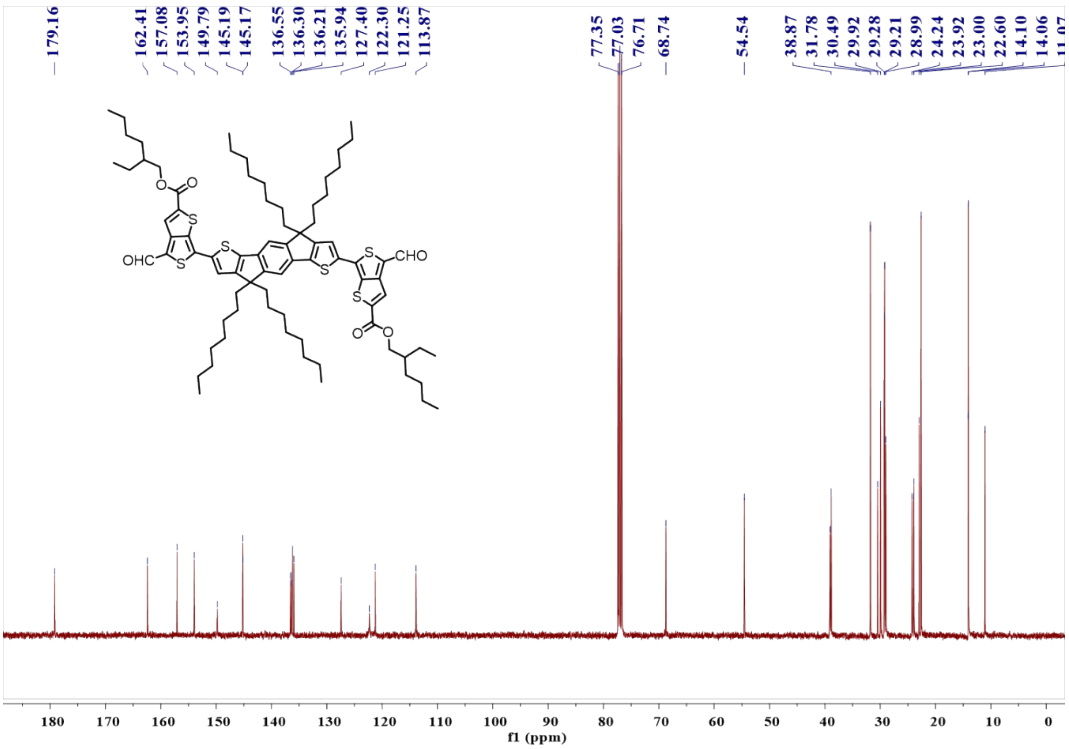

Fig. S12. ^{13}C NMR spectrum of **compound 5b**.

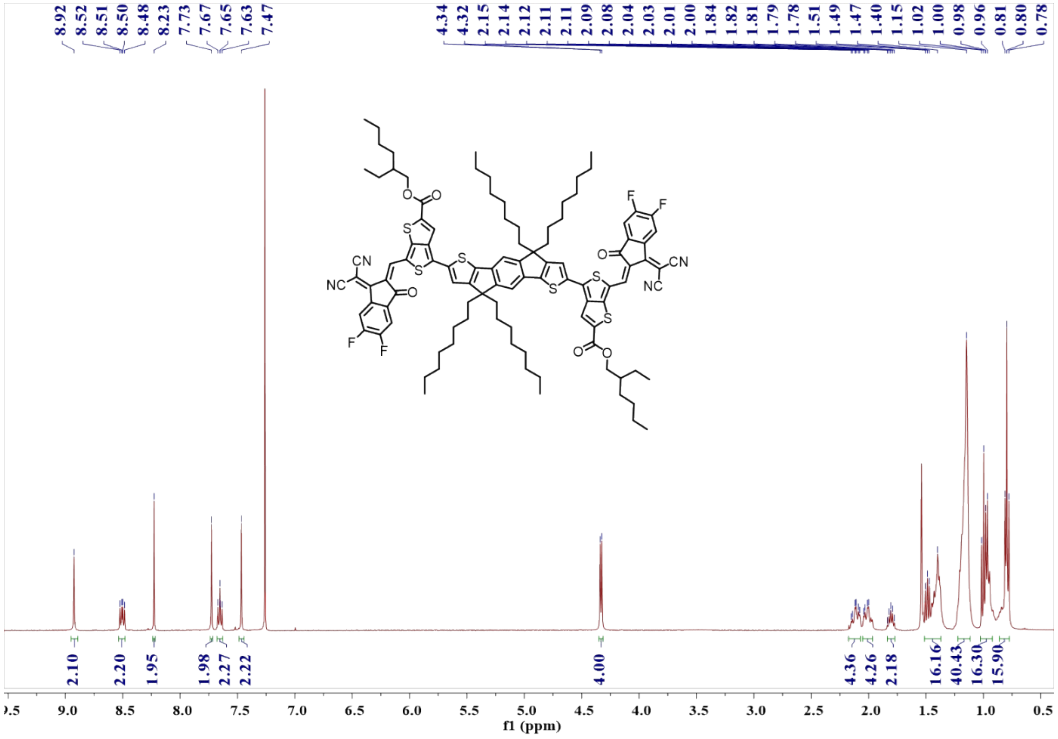

Fig. S13. ^{1}H NMR spectrum of **6T4F**.

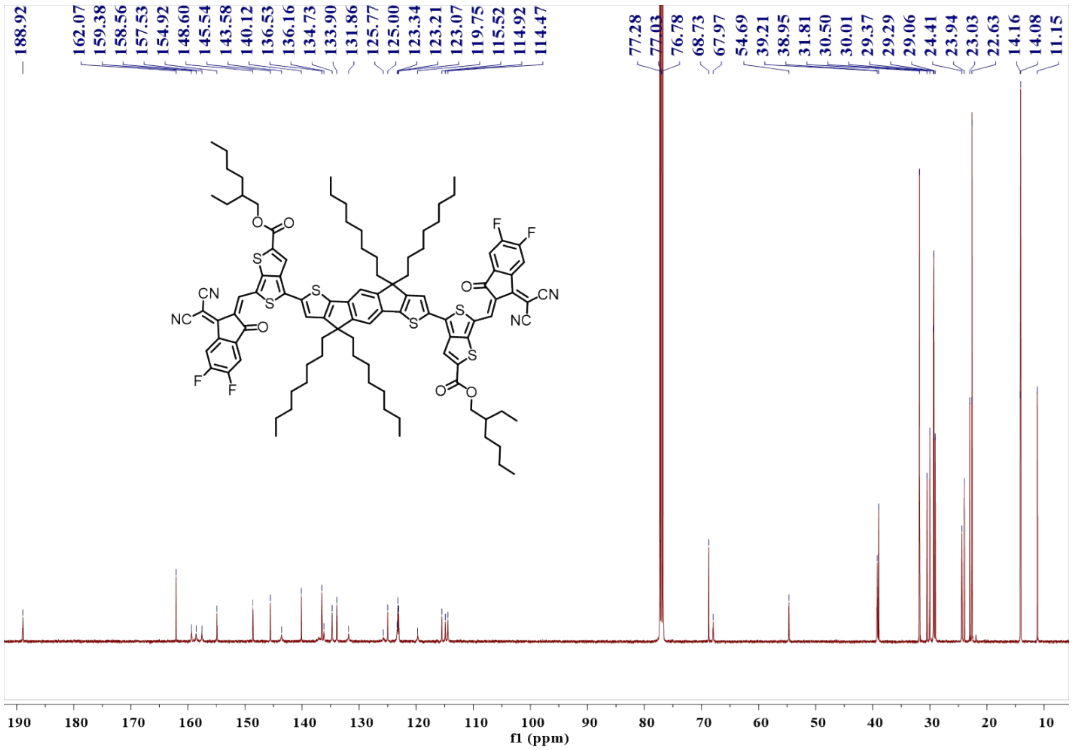

Fig. S14. ^{13}C NMR spectrum of **6T4F**.

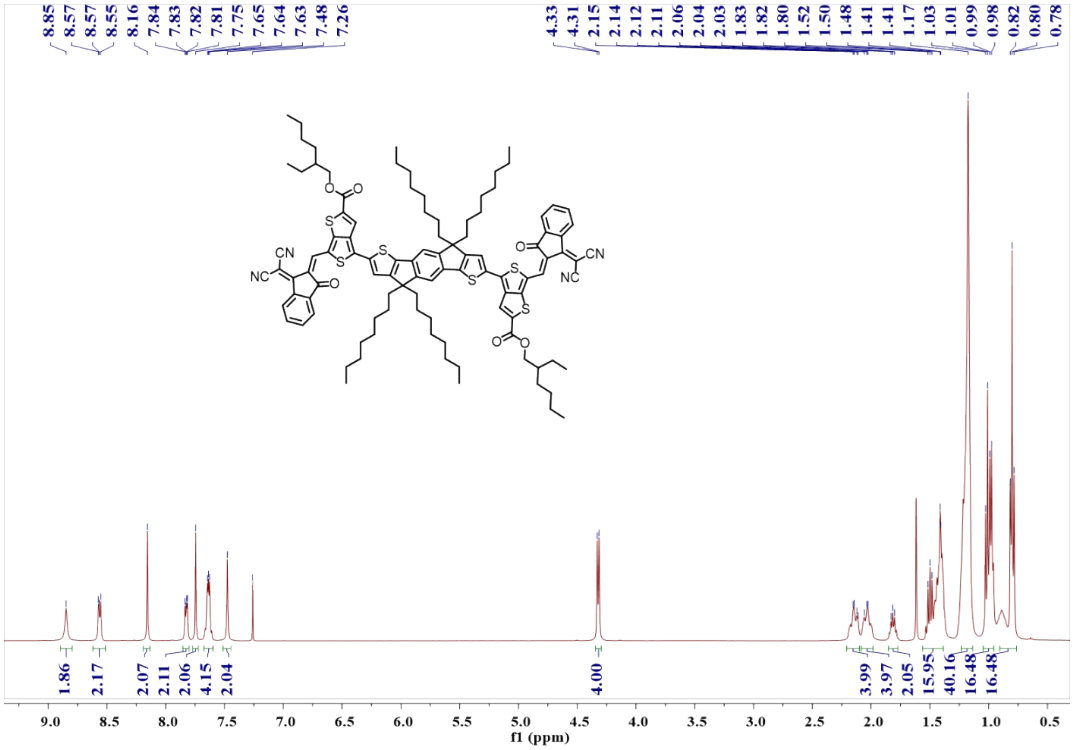

Fig. S15. ^{1}H NMR spectrum of **6TIC**.

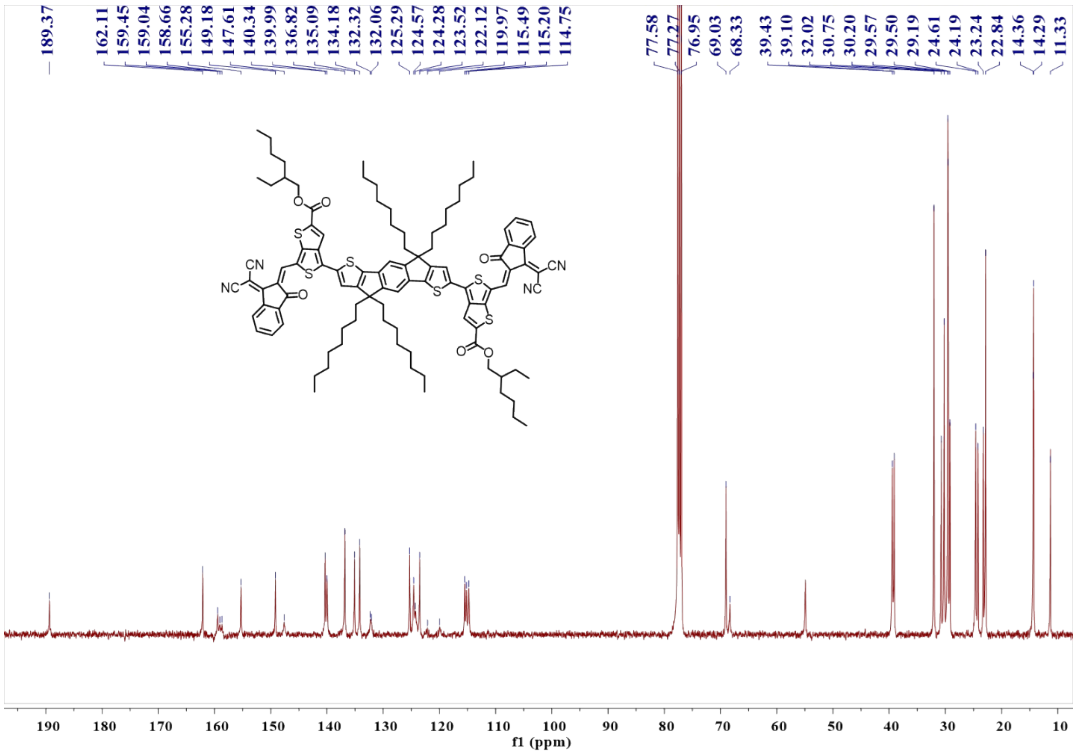

Fig. S16. ^{13}C NMR spectrum of **6TIC**.

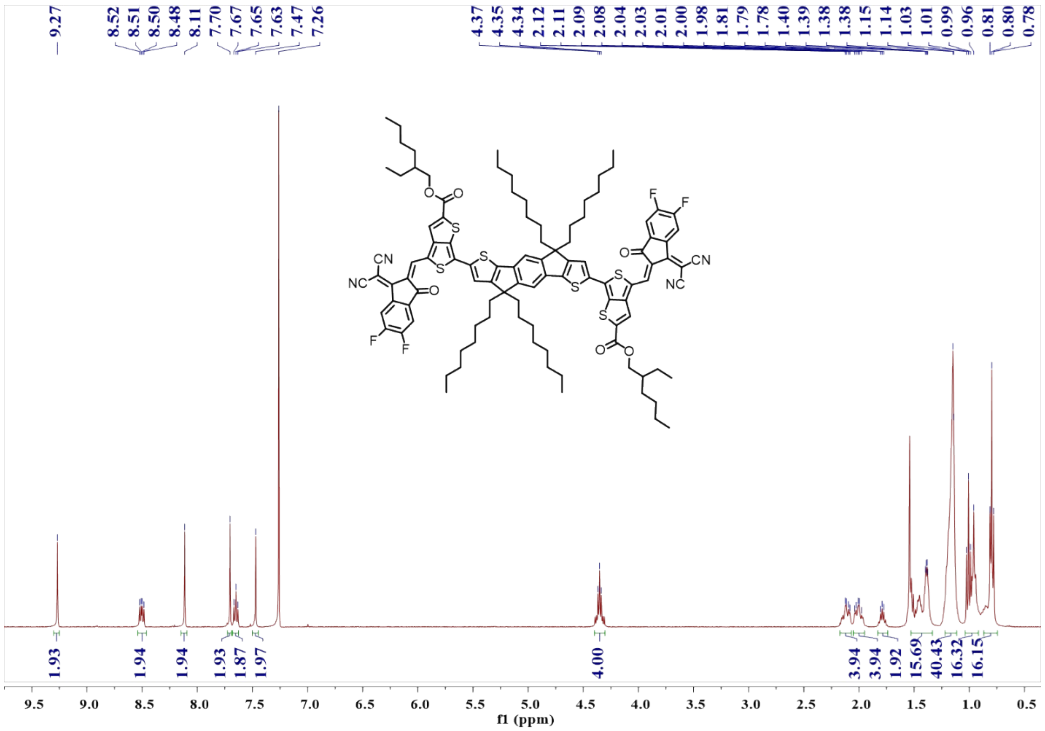

Fig. S17. ^{1}H NMR spectrum of **4T4F**.

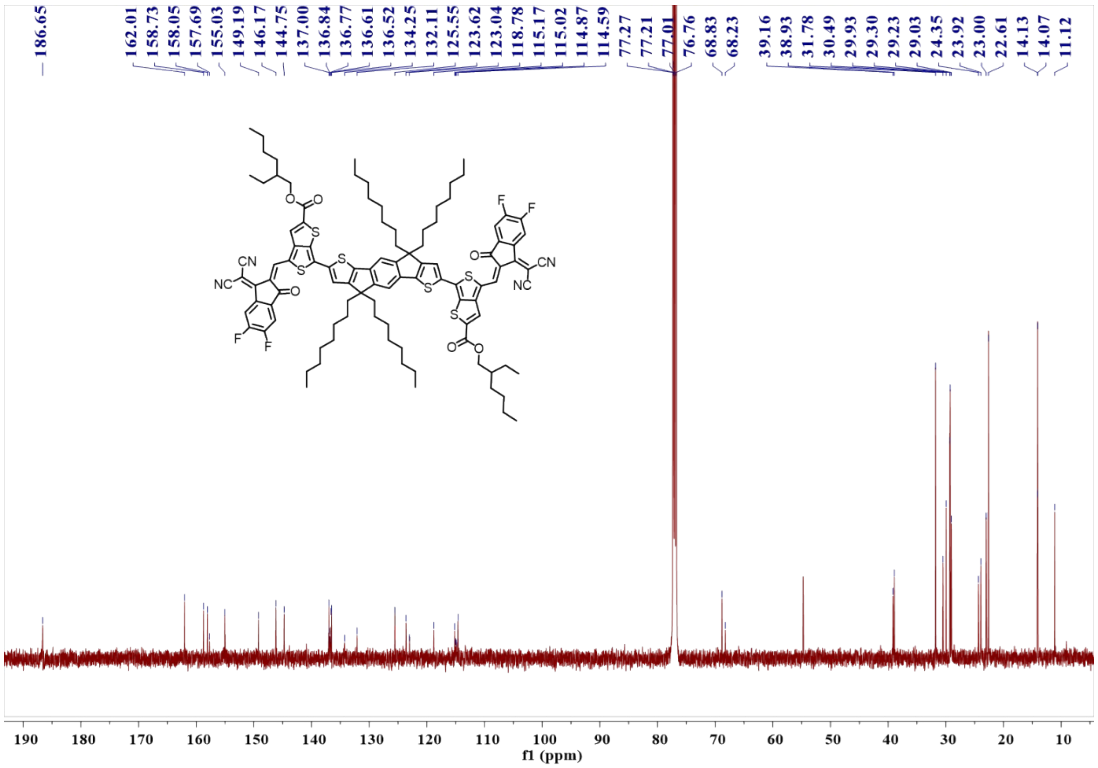

Fig. S18. ^{13}C NMR spectrum of **4T4F**.

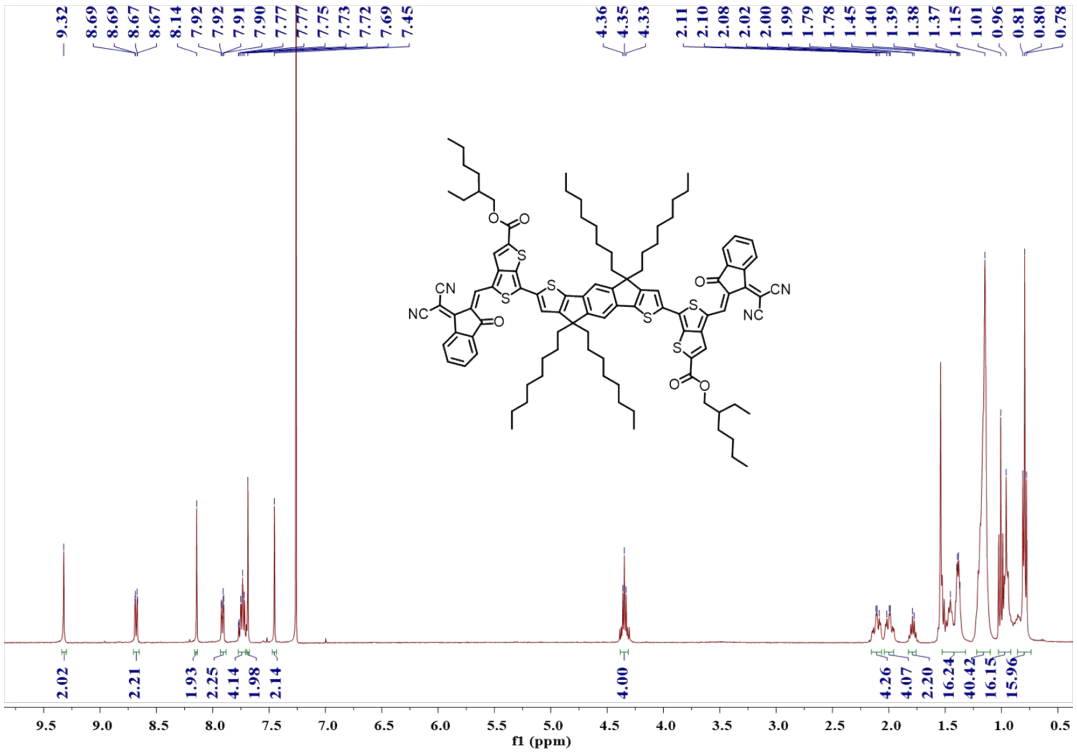

Fig. S19. ^{1}H NMR spectrum of **4TIC**.

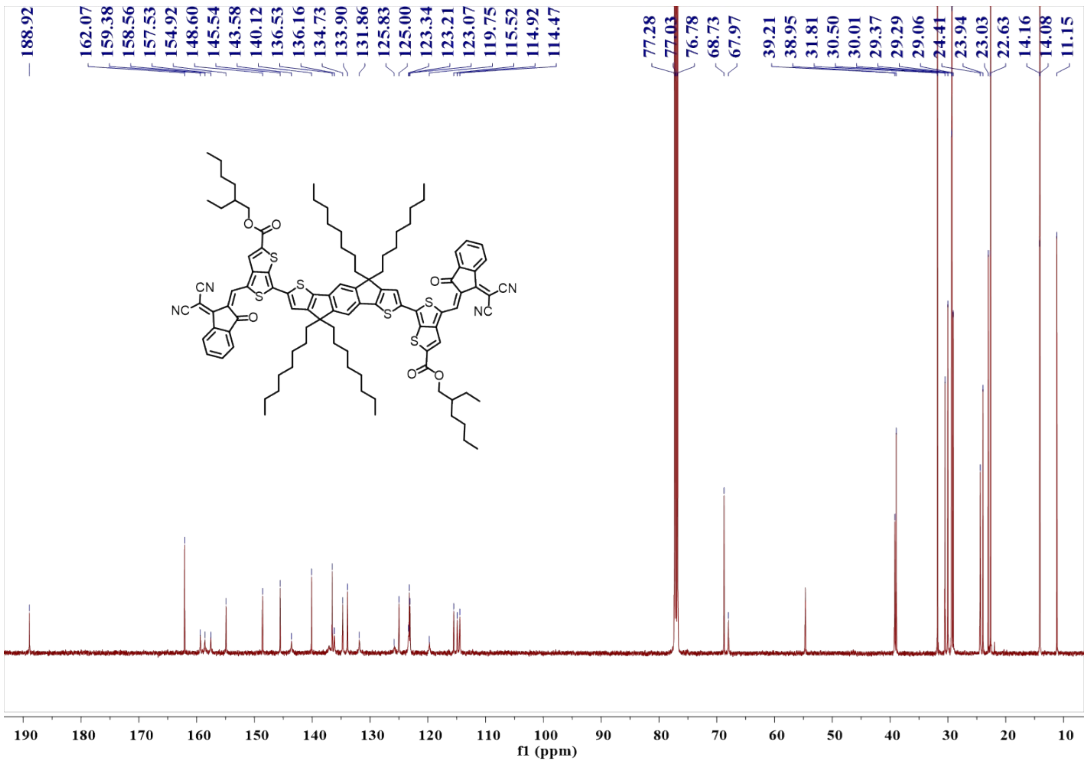

Fig. S20. ^{13}C NMR spectrum of **4TIC**.

1. P. Brogdon, F. Giordano, G. A. Puneky, A. Dass, S. M. Zakeeruddin, M. K. Nazeeruddin, M. Gratzel, G. S. Tschumper and J. H. Delcamp, *Chem. Eur. J.*, 2016, **22**, 694-703.